Dispersive measurement of spin shot noise in a Bose-Einstein condensate

Kosuke Shibata [1,2,*] Naota Sekiguchi [3] Junnosuke Takai [4] and Takuya Hirano [1]
[1] Department of Physics, Gakushuin University, Tokyo 171-8588, Japan
[2] Department of Physics, Graduate School of Science, Kyoto University, Kyoto 606-8502, Japan
[3] Department of Electrical and Electronic Engineering, Institute of Science Tokyo, Tokyo 152-8550, Japan
[4] National Metrology Institute of Japan, National Institute of Advanced Industrial Science and Technology, Ibaraki 305-8563, Japan

(Received 28 January 2025; accepted 19 September 2025; published 14 October 2025)

We report dispersive spin shot noise measurement of a Bose-Einstein condensate (BEC). While dispersive probing has been used for quantum spin noise measurement of thermal and cold gases for decades, confirmative measurement of shot noise of real spin, i.e., the linear dependence of the spin variance on the number of atoms in a BEC, has been lacking. Here, we demonstrate precise spin noise measurement of a BEC of rubidium atoms at the spin shot noise level by polarization rotation using a two-color probe at optimal detunings, with power balance stabilization to suppress probe-induced excess spin noise. This work opens the possibility for the unexplored study of quantum spin fluctuations in multicomponent or spinor BECs and offers an approach to improve spin measurement precision, which is relevant to atomic spin-based sensors.

DOI: 10.1103/md2j-t2qq

I. INTRODUCTION

Spin, an inherently quantum mechanical quantity, now plays an important role in cutting-edge applications, including quantum information processing and quantum computation [1–4]. It can also serve as a high-precision quantum sensor [5]. For example, atomic vapor is one of the most sensitive magnetometers with a sensitivity down to sub-fT/$\sqrt{\text{Hz}}$ [6,7]. A cold atomic gas, especially a Bose-Einstein condensate (BEC), is a good candidate for a spatially resolved magnetometer [8–11]. It has been pointed out that a tightly confined single-domain BEC can achieve an energy resolution, which is a measure of the magnetic field sensitivity obtainable with a given measurement volume, of better than $\hbar$ [12], exceeding the limit for superconducting quantum interference devices [13,14].

Precise spin measurement is a key ingredient for the aforementioned applications. A challenge in spin measurement is to achieve sensitivity at the standard quantum limit (SQL), the minimum sensitivity attainable with quantum-mechanically uncorrelated probes (atoms in the context here) [15–17]. As the SQL is proportional to $1/\sqrt{N}$, where N is the number of probes [18], it can be easily hindered by technical noise, particularly for a large system. Nevertheless, the spin shot noise for atomic gases has been measured and even entanglement or spin squeezing induced by measurement has been reported for hot [19–22] and cold [23–27] gases. Spin squeezing by cavity-aided measurements [28,29] demonstrated remarkable achievements, including a practical metrological enhancement [30–32]. Squeezing of a pseudospin consisting of two hyperfine sublevels (atom number squeezing) of a BEC has been observed with an absorptive atom number measurement [33–35]. However, confirmative evidence of successful shot noise measurement of real spin, i.e., the linear increase of the spin variance with respect to the atom number, has not been observed for a BEC.

Spin measurement of a BEC at the SQL level will open an avenue in the study of multicomponent or spinor BECs [36], in addition to the pursuit of the best measurement precision. The observation of quantum spin fluctuations will help to experimentally explore the fundamental aspects of BECs, as did precise atom number measurements at the shot noise level [37], where a sudden increase of fluctuations at the critical temperature [38,39] was observed. For example, spin squeezing in the spatially extended field [40] may be explored. Dispersive spin probing is superior to absorptive probing, which is more common in cold atom experiments, in that it allows *in situ* and consecutive spin measurement, offering the possibility to track the spin dynamics. While entanglement structure in a spinor BEC was detected by sophisticated absorption imaging [41], the dispersive spin probing may reveal the evolution of such structure.

Polarization rotation detection, one of the most popular dispersive spin probing techniques, is also attractive in the context of quantum nondemolition (QND) spin measurement [42,43]. Traditionally, measurement-induced spin squeezing of a cold gas has been demonstrated with the use of a cigar-shaped gas in an elongated optical trap [23,25–27], which is advantageous for significant squeezing [44,45]. For a BEC, a large atom-field interaction may be achieved without a cigar-shaped configuration due to its high atomic density. Therefore, dispersive spin BEC measurement may enable

*Contact author: shibata@qo.phys.gakushuin.ac.jp

quantum-enhanced sensing in a small volume. Improving the sensitivity of spin measurement will lead to breaking of the conventional magnetic field sensitivity limit in the micrometer scale and shed light on the open question of the energy resolution limit [46].

We report the measurement of spin noise of a BEC by polarization rotation. A two-color probe with stabilized power balance was used to suppress the nonlinear ac Stark shift, which can be a dominant technical noise source in spin shot noise measurements of BECs with a relatively small number of atoms. The frequencies of two probe fields were optimized to reduce atom loss due to light-assisted collisions, which tends to be significant in probing BECs due to their high atomic density. A charged-coupled device (CCD) camera was used in the spin noise measurements to observe the polarization rotation instead of a balanced photodiode detector, which has often been used to achieve shot-noise-level sensitivity [47,48]. The camera naturally offers the ability to perform spatially resolved measurements and will enable the exploration of the spatial properties of the spin noise distribution, while the spatial resolution is not fully utilized in this work. The camera also offers the advantage of good effective spatial mode matching between atoms and probes when combined with postselection of the region of interest. We observed a linear increase in the variance of the polarization rotation angle with respect to atom number, indicating successful observation of spin shot noise and realization of precise spin noise measurement at the SQL.

II. EXPERIMENTAL METHOD

A. Preparation of atoms

We measured the spin noise for a BEC in a crossed optical dipole trap. Atoms were loaded into the trap from a magnetic trap and evaporatively cooled to produce an almost pure BEC in the $|f = 2, m_z = +2\rangle$ state of up to 3×10^5 atoms, where the quantized axis z is defined by the direction of the bias magnetic field B [see Fig. 1(a)]. The typical radial and axial trap frequencies of the optical trap after the final stage of the evaporation were 113(2) and 34(2) Hz, respectively. The bias magnetic field was set to 29.5 μT during the spin noise measurements. The bias field was sufficiently larger than the drift of the environmental magnetic field along the x axis (typically 20 nT over a night), suppressing the variation in the spin direction due to the fluctuation of B_x during data acquisition. We also performed spin cleaning with a microwave transition and hyperfine-state-selective blast light to ensure an initial spin polarization.

B. Laser system

The probe consists of two (main and compensation) beams near the D1 line at 795 nm [49], as described below. The main beam frequency was stabilized using the modulation transfer spectroscopy signal of a magnetically shielded rubidium cell with detuning from atomic resonance produced by acousto-optic modulators (AOMs). The compensation beam was frequency-offset locked to the main beam for flexible detuning. The two beams were combined and coupled into a common single-mode optical fiber for spatial beam mode matching. They also passed through a common AOM for pulsing beams. The probe passed through a polarizer and a quarter wave plate (QWP) for compensation of polarization ellipticity before the atom cell.

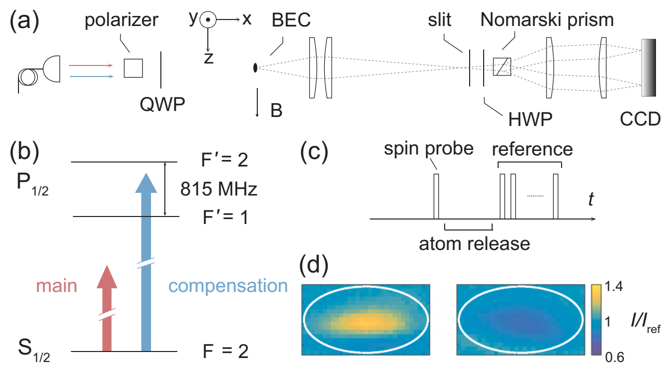

FIG. 1. Experimental setup. (a) Spin detection system. The polarization rotation for the two-color probe linearly polarized along the z axis is detected by the CCD camera. (b) Relevant energy levels of ^{87}Rb and probe beam frequencies. (c) Time sequence of the probing pulses. (d) Images of orthogonal polarization components for a BEC with a spin direction along the x axis. The measured intensity I normalized against the reference intensity $I_{\rm ref}$ is shown. The white ellipse represents the boundary of the region of interest. The lengths of the major and minor axes of the ellipse are 17 and 9 μm, respectively.

C. Spin detection

We estimated the collective spin component, F_x, from the polarization rotation of the probe light. The polarization rotation angle was measured by a polarimeter consisting of a half wave plate, a Nomarski prism, and a CCD camera capable of kinetic imaging (PIXIS1024BR, Princeton Instruments). The polarization rotation was analyzed within an elliptic region that covers the atoms sufficiently. In order to observe the spin shot noise without being hindered by photon shot noise, it was important to set the analysis region as small as possible.

The rotation angle of polarization plane was given by an angle $\theta = gF_x$, where g is the coupling strength determined by the atomic optical density and the probe frequency, due to the paramagnetic Faraday rotation effect. The variance of the polarization angle is given by

$$\mathrm{Var}(\theta) = aN + bN^2 + \mathrm{Var}(\theta)_0, \tag{1}$$

where $\mathrm{Var}(\theta)_0$ is the variance in the absence of atoms, including the variance due to photon shot noise, given by $1/(4N_{\rm p})$, with $N_{\rm p}$ being the number of probe photons, and the readout noise. The first and second terms on the right-hand side of Eq. (1) denote the spin shot noise and the technical noise, respectively, with different dependences on the atom number N. Because we probed atoms in the coherent spin state, the spin shot noise term should be $g^2 f|\langle N_{\rm eff}^{(2)}\rangle|/2$, where $N_{\rm eff}^{(2)}$ represents the effective atom number determined by the geometry of the atoms and the probe [45].

D. Probe parameter optimization

Probe-induced spin change is one of the dominant types of technical noise sources in spin measurements. This is particularly true in our spin shot noise measurements of a BEC. Measuring spin shot noise for a small number of atoms requires a large probe photon number to reduce uncertainties due to photon shot noise in polarization rotation measurements, thus increasing probe-induced spin changes. For a quantitative discussion, we introduce the ratio of the spin shot noise of the coherent spin state (without consideration of the detection geometry [45]) to the photon shot noise resolution in the polarization rotation measurement [50], $\xi = 4g^2NN_\mathrm{p}$. A larger ξ is better for spin shot noise measurements. As the coupling strength g scales to $(A\delta)^{-1}$, where A is the measurement cross section and δ is the detuning from the resonance (a two-level model is assumed here for simplicity), ξ can be written as

$$\xi = 4\tilde{g}^2\frac{N}{A}\frac{N_\mathrm{p}}{A\delta^2}, \qquad (2)$$

where $\tilde{g}$ is the normalized coupling strength, independent of A and δ. Spin shot noise measurements of an atom cloud of small column atom density (N/A) require a large $N_\mathrm{p}/(A\delta^2)$, which causes large photoinduced atom loss, photon scattering, and light shift. Spin-dependent light shift due to vector and tensor atom-field interaction is harmful for precise spin measurement, as explained below. The column atom density is not high in our measurement configuration where a BEC is probed along its radial direction, while the configuration is compatible with spatially resolved magnetometry [11]. Therefore, we make efforts to reduce the spin-dependent light shift.

1. Polarization optimization

The vector light shift or "fictitious magnetic field" acts in the same manner as a magnetic field along the probe propagation axis and causes instantaneous spin rotation during the probe pulse. It increases technical noise in a spin measurement when combined with shot-to-shot fluctuations of the probe intensity and magnetic field. We suppress the vector light shift by reducing the ellipticity of the probe. Such a reduction is often optimized by spectroscopy with atoms themselves [51,52]. Spectroscopy is, however, less sensitive here because the fictitious field is orthogonal to the bias magnetic field. We instead directly measured the spin change due to three probe pulses of 1 μs with an interval of the Larmor precession using spin-resolved absorption imaging [53], from which we measured the magnetization along the z axis. A $\pi/2$ pulse was applied after probe irradiation to maximize the sensitivity to the spin rotation due to the vector shift around the total magnetic field almost along the z axis. We adjusted the QWP angle to minimize the magnetization change before obtaining the experimental data presented below.

2. Two-color probe

The linearly polarized probe caused spin evolution by nonlinear light shift (proportional to the square of the magnetic quantum number) due to the tensor term of the atom-field interaction. Several techniques have been developed to reduce nonlinear spin evolution, such as magic angle probing of rotating spin [54], alternating polarization probe for a ^{87}Rb thermal gas in the $F = 1$ state [55], and two-color probing for Cs of $F = 4$ [27].

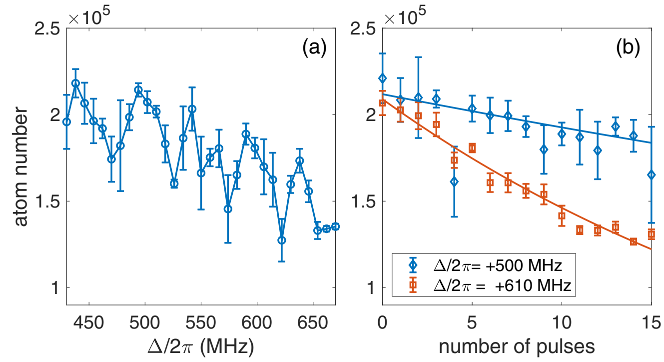

FIG. 2. Loss by the compensation beam. (a) Loss dependence on the detuning. We applied five pulses with 1 μs width and peak power of 180 μW. (b) Loss rate measurement results. The blue diamonds and red squares represent the remaining atom number after irradiating by compensation beam pulses of $\Delta/(2\pi) = +500$ and $+610$ MHz, respectively. The pulse width is 1 μs. The peak power is 180 μW. The solid lines are exponential fits to the data.

If the probe polarization vector perfectly coincided with the atomic spin polarization, it would only induce a phase shift on a single magnetic sublevel ($|F = 2, m_z = +2\rangle$ in our case) and cause no nonlinear spin evolution. In practice, however, it is difficult to sufficiently eliminate the nonlinear spin evolution by this polarization matching strategy. For example, fluctuation of the direction of the bias magnetic field defining the spin quantization axis and slow change of light polarization increase the polarization rotation variance. Inhomogeneity of the light polarization over the atom cloud may limit the suppression of the nonlinear evolution.

We adopted a two-color probe to sufficiently suppress nonlinear spin evolution. We combined a beam with red detuning from the $F = 2 - F' = 1$ transition (main beam) and another beam with its frequency between the $F = 2 - F' = 1$ and $F = 2 - F' = 2$ transitions (compensation beam) [see Fig. 1(b)]. The total nonlinear shift caused by these beams can be canceled by adjusting the beam power balance [49]. The power ratio of the main and compensation beams was stabilized to yield an instability of less than 0.01.

Before performing measurements with the two-color probe, we performed loss spectroscopy with the compensation beam to find its optimal detuning. We found several frequencies with smaller atom loss rates, as shown in Fig. 2(a). Figure 2(b) shows the loss rates at certain frequencies. The atoms in the $F = 1$ state were removed by a beam resonant to the $F = 1 - F' = 0$ D_2 transition after each probe pulse in these measurements. We observed the loss rate reduction by the $F = 1$ removal, which is attributed to the suppression of hyperfine Raman superradiant scattering [9]. The atom number after n pulses was fitted by $N^{(n)} = N^{(0)}\exp(-\gamma n)$, where $N^{(0)}$ is the initial atom number. The loss rates γ by the beams of $\Delta/(2\pi) = +500$ and $+610$ MHz were 0.009(2) and 0.036(2), respectively. We set the compensation beam detuning to $+500$ MHz in the following experiments.

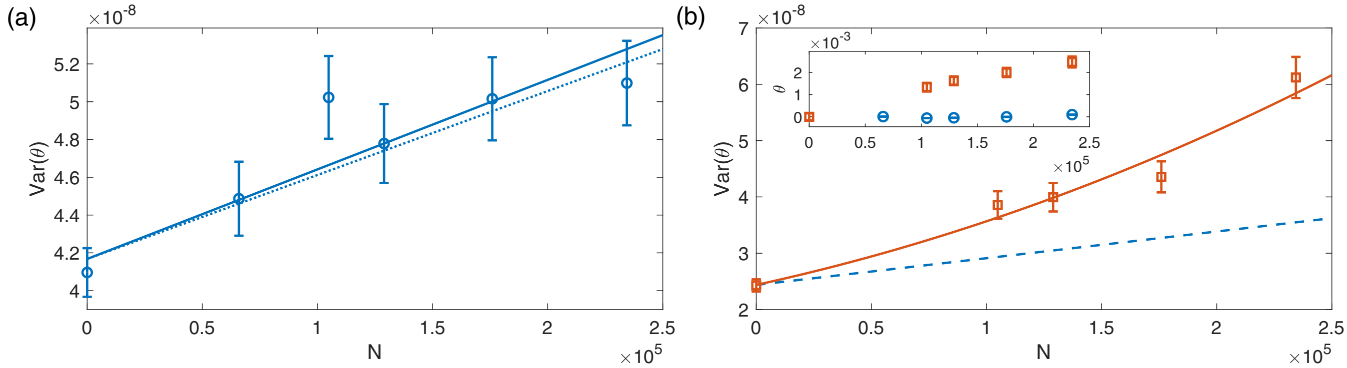

FIG. 3. Spin noise measurement. (a) Variance of θ vs the atom number for the measurement with the two-color probe. The blue solid line is a linear fit to the measurement data (blue circles). The dotted line represents the estimation from the coupling strength g (see the main text). (b) Variance of θ without the compensation beam. The red solid line is a quadratic fit to the measurement data (red squares). The reference noise level with the same slope as panel (a) is also plotted (blue dashed line). The offset of the reference is adjusted to that of the red solid line. The error bars represent the statistical uncertainties of the variance. The inset shows the polarization rotation angle with (blue circles) and without (red squares) the compensation beam.

Although we found the optimal compensation beam frequency, the optimal compensation beam still induces a larger atom loss than the optimally red-detuned main beam [11]. This is probably because the light-assisted collisional loss is not sufficiently suppressed for the compensation beam, the frequency of which is close to the atomic resonances, and, more importantly, is blue detuned from the $F = 2 - F' = 1$ transition with a continuous loss spectrum [56]. The compensation beam red detuned from the D_2 line may be used for a lower loss rate.

III. SPIN SHOT NOISE MEASUREMENT

We performed repeated measurements of the polarization rotation of the probe passing the BEC in the optical trap to deduce the spin noise. To avoid an increase in noise due to the measured slow polarization rotation angle fluctuation correlated with the room temperature change, we took reference images just after probing the atoms [see Fig. 1(c)] and used a net polarization rotation θ due to the atoms, calculated by $\theta_{\mathrm{w/atom}} - \theta_{\mathrm{w/oatom}}$, where $\theta_{\mathrm{w/atom}}$ represents the estimated polarization rotation angle for a camera image with atoms and $\theta_{\mathrm{w/oatom}}$ is the average of the estimated angles over the reference frames, for the noise analysis. The polarization rotation angle was estimated from the vertically and horizontally polarized probe photon numbers, N_{V} and N_{H}, in the region of interest of the imaging camera shown in Fig. 1(d) as $(N_{\mathrm{V}} - N_{\mathrm{H}})/2(N_{\mathrm{V}} + N_{\mathrm{H}})$.

The variance of θ, Var(θ), was measured for a BEC of several groups of different mean atom numbers with the two-color probe. The main and compensation beam detunings were -840 and $+500$ MHz in this measurement. The main probe beam detuning was set to reduce the light-assisted collisional atom loss [11]. Their power ratio was stabilized to 8.57 : 1. The total photoelectron number detected by the camera in the region of interest was 7.8×10^6 per pulse. The atom number was controlled by changing the final rf frequency for forced evaporation in the magnetic trap. The measured Var(θ) shown in Fig. 3(a) was fitted by a linear function with a slope of $4.7(9) \times 10^{-14}$. No significant quadratic increase in the variance was observed. This result indicates that we measured the spin noise at the shot-noise-limited level. It should be noted that Var(θ) for each atom number group was obtained from more than 1000 experimental runs over approximately 11 h. Repeated atom probing in a single experiment cycle [24,25] was not applied because we observed that a longer interval between the signal and reference frames increased the measured photon noise, which was probably due to vibration of the imaging system. We nevertheless observed no significant excess spin noise, implying that the measurement scheme is robust.

The observed atomic noise level is compared with the theoretical prediction. The spin shot noise is given by $\sum_i r_i g_i^2 N_{\mathrm{eff}}^{(2)}/4$, where r_i is the power ratio of main ($i = 1$) and compensation ($i = 2$) beams and g_i is the polarization rotation per effective atom number $N_{\mathrm{eff}}^{(1)}$. $N_{\mathrm{eff}}^{(1)}$ and $N_{\mathrm{eff}}^{(2)}$ are effective atom numbers calculated from the probe beam mode and the atomic density distribution [45]. Approximating the probe beam mode by a fundamental Gaussian one, we estimate $N_{\mathrm{eff}}^{(1)}$ and $N_{\mathrm{eff}}^{(2)}$ to be $0.69N$ and $0.51N$, respectively. g_1 and g_2 are determined to be 4.2×10^{-7} and -2.8×10^{-7} from the atom number measured by the absorption imaging and the polarization rotation angle with the spin directed along the x axis. Combining these values, the slope is estimated to be 4.4×10^{-14}, in good agreement with the experimental observation.

We present the polarization measurement results with the main beam only to clarify the effect of the compensation beam. To enhance the spin change due to the probe with limited available power, we used a metapulse consisting of two pulses with the interval set to the Larmor period, giving almost twice as many photoelectrons as the usual pulse. A variance due to atoms larger than that for the two-color probe was observed. The measured variance was fitted by a quadratic function $p_2N^2 + p_1N + p_0$. The excess noise was attributed to the nonlinear polarization rotation. The change in the rotation angle θ itself due to atoms was observed, while θ for the two-color probe remained constant irrespective of the atom number, as shown in the inset of Fig. 3(b). $\theta \sim 10^{-3}$ implies that atom number fluctuation or a beam power imbalance of 10% would result in an excess variance of θ of 10^{-8} rad^2 and prohibit shot-noise-limited spin measurements without the compensation beam.

IV. CONCLUSIONS

To conclude, we performed spin noise measurements of a BEC of ^{87}Rb atoms trapped in an optical dipole trap by polarization rotation of a two-color probe. Optimization of the probe frequency and polarization, and beam power balance stabilization were performed to reduce probe-induced excess noises in the polarization rotation measurement. We observed a linear increase in the polarization rotation variance with respect to the atom number, which is characteristic of spin shot noise. The demonstrated precise spin noise measurements can be used to experimentally explore the fundamental quantum properties of multi-spin-component or spinor BECs. Precise and shot-noise-limited spin measurements are also key to improving BEC magnetometry.

ACKNOWLEDGMENTS

This work was supported by MEXT Quantum Leap Flagship Program (MEXT Q-LEAP) Grant No. JPMXS0118070326, JSPS KAKENHI Grant No. JP22K03496, and the Asahi Glass Foundation (AGC).

DATA AVAILABILITY

The data that support the findings of this article are not publicly available upon publication because it is not technically feasible and/or the cost of preparing, depositing, and hosting the data would be prohibitive within the terms of this research project. The data are available from the authors upon reasonable request.

[1] T. F. Watson, S. G. J. Philips, E. Kawakami, D. R. Ward, P. Scarlino, M. Veldhorst, D. E. Savage, M. G. Lagally, M. Friesen, S. N. Coppersmith, M. A. Eriksson, and L. M. K. Vandersypen, A programmable two-qubit quantum processor in silicon, Nature (London) **555**, 633 (2018).

[2] F. Arute, K. Arya, R. Babbush, D. Bacon, J. C. Bardin, R. Barends, R. Biswas, S. Boixo, F. G. S. L. Brandao, D. A. Buell *et al.*, Quantum supremacy using a programmable superconducting processor, Nature (London) **574**, 505 (2019).

[3] X. Xue, B. Patra, J. P. G. van Dijk, N. Samkharadze, S. Subramanian, A. Corna, B. Paquelet Wuetz, C. Jeon, F. Sheikh, E. Juarez-Hernandez *et al.*, CMOS-based cryogenic control of silicon quantum circuits, Nature (London) **593**, 205 (2021).

[4] K. Barnes, P. Battaglino, B. J. Bloom, K. Cassella, R. Coxe, N. Crisosto, J. P. King, S. S. Kondov, K. Kotru, S. C. Larsen *et al.*, Assembly and coherent control of a register of nuclear spin qubits, Nat. Commun. **13**, 2779 (2022).

[5] C. L. Degen, F. Reinhard, and P. Cappellaro, Quantum sensing, Rev. Mod. Phys. **89**, 035002 (2017).

[6] I. K. Kominis, T. W. Kornack, J. C. Allred, and M. V. Romalis, A subfemtotesla multichannel atomic magnetometer, Nature (London) **422**, 596 (2003).

[7] H. B. Dang, A. C. Maloof, and M. V. Romalis, Ultrahigh sensitivity magnetic field and magnetization measurements with an atomic magnetometer, Appl. Phys. Lett. **97**, 151110 (2010).

[8] S. Wildermuth, S. Hofferberth, I. Lesanovsky, E. Haller, L. M. Andersson, S. Groth, I. Bar-Joseph, P. Krüger, and J. Schmiedmayer, Microscopic magnetic-field imaging, Nature (London) **435**, 440 (2005).

[9] M. Vengalattore, J. M. Higbie, S. R. Leslie, J. Guzman, L. E. Sadler, and D. M. Stamper-Kurn, High-resolution magnetometry with a spinor Bose-Einstein condensate, Phys. Rev. Lett. **98**, 200801 (2007).

[10] F. Yang, A. J. Kollár, S. F. Taylor, R. W. Turner, and B. L. Lev, Scanning quantum cryogenic atom microscope, Phys. Rev. Appl. **7**, 034026 (2017).

[11] N. Sekiguchi, K. Shibata, A. Torii, H. Toda, R. Kuramoto, D. Fukuda, and T. Hirano, Sensitive spatially resolved magnetometry using a Bose-condensed gas with a bright probe, Phys. Rev. A **104**, L041306 (2021).

[12] S. P. Alvarez, P. Gomez, S. Coop, R. Zamora-Zamora, C. Mazzinghi, and M. W. Mitchell, Single-domain Bose condensate magnetometer achieves energy resolution per bandwidth below $\hbar$, Proc. Natl. Acad. Sci. USA **119**, e2115339119 (2022).

[13] R. H. Koch, D. J. Van Harlingen, and J. Clarke, Quantum-noise theory for the resistively shunted Josephson junction, Phys. Rev. Lett. **45**, 2132 (1980).

[14] R. H. Koch, D. J. Van Harlingen, and J. Clarke, Quantum noise theory for the dc SQUID, Appl. Phys. Lett. **38**, 380 (1981).

[15] V. Giovannetti, S. Lloyd, and L. Maccone, Quantum metrology, Phys. Rev. Lett. **96**, 010401 (2006).

[16] S. Boixo, S. T. Flammia, C. M. Caves, and J. Geremia, Generalized limits for single-parameter quantum estimation, Phys. Rev. Lett. **98**, 090401 (2007).

[17] L. Pezzè, A. Smerzi, M. K. Oberthaler, R. Schmied, and P. Treutlein, Quantum metrology with nonclassical states of atomic ensembles, Rev. Mod. Phys. **90**, 035005 (2018).

[18] S. L. Braunstein and C. M. Caves, Statistical distance and the geometry of quantum states, Phys. Rev. Lett. **72**, 3439 (1994).

[19] B. Julsgaard, A. Kozhekin, and E. S. Polzik, Experimental long-lived entanglement of two macroscopic objects, Nature (London) **413**, 400 (2001).

[20] G. Vasilakis, H. Shen, K. Jensen, M. Balabas, D. Salart, B. Chen, and E. S. Polzik, Generation of a squeezed state of an oscillator by stroboscopic back-action-evading measurement, Nat. Phys. **11**, 389 (2015).

[21] H. Bao, J. Duan, S. Jin, X. Lu, P. Li, W. Qu, M. Wang, I. Novikova, E. E. Mikhailov, K.-F. Zhao, K. Mølmer, H. Shen, and Y. Xiao, Spin squeezing of 10^{11} atoms by prediction and retrodiction measurements, Nature (London) **581**, 159 (2020).

[22] J. Kong, R. Jiménez-Martínez, C. Troullinou, V. G. Lucivero, G. Tóth, and M. W. Mitchell, Measurement-induced, spatially-extended entanglement in a hot, strongly-interacting atomic system, Nat. Commun. **11**, 2415 (2020).

[23] J. Appel, P. J. Windpassinger, D. Oblak, U. B. Hoff, N. Kjaergaard, and E. S. Polzik, Mesoscopic atomic entanglement

for precision measurements beyond the standard quantum limit, Proc. Natl. Acad. Sci. USA **106**, 10960 (2009).
[24] T. Takano, M. Fuyama, R. Namiki, and Y. Takahashi, Spin squeezing of a cold atomic ensemble with the nuclear spin of one-half, Phys. Rev. Lett. **102**, 033601 (2009).
[25] R. J. Sewell, M. Koschorreck, M. Napolitano, B. Dubost, N. Behbood, and M. W. Mitchell, Magnetic sensitivity beyond the projection noise limit by spin squeezing, Phys. Rev. Lett. **109**, 253605 (2012).
[26] G. Colangelo, F. M. Ciurana, L. C. Bianchet, R. J. Sewell, and M. W. Mitchell, Simultaneous tracking of spin angle and amplitude beyond classical limits, Nature (London) **543**, 525 (2017).
[27] D. Hemmer, E. Montaño, B. Q. Baragiola, L. M. Norris, E. Shojaee, I. H. Deutsch, and P. S. Jessen, Squeezing the angular momentum of an ensemble of complex multilevel atoms, Phys. Rev. A **104**, 023710 (2021).
[28] Y. Colombe, T. Steinmetz, G. Dubois, F. Linke, D. Hunger, and J. Reichel, Strong atom–field coupling for Bose–Einstein condensates in an optical cavity on a chip, Nature (London) **450**, 272 (2007).
[29] F. Brennecke, T. Donner, S. Ritter, T. Bourdel, M. Köhl, and T. Esslinger, Cavity QED with a Bose–Einstein condensate, Nature (London) **450**, 268 (2007).
[30] K. C. Cox, G. P. Greve, J. M. Weiner, and J. K. Thompson, Deterministic squeezed states with collective measurements and feedback, Phys. Rev. Lett. **116**, 093602 (2016).
[31] O. Hosten, N. J. Engelsen, R. Krishnakumar, and M. A. Kasevich, Measurement noise 100 times lower than the quantum-projection limit using entangled atoms, Nature (London) **529**, 505 (2016).
[32] B. Braverman, A. Kawasaki, E. Pedrozo-Peñafiel, S. Colombo, C. Shu, Z. Li, E. Mendez, M. Yamoah, L. Salvi, D. Akamatsu, Y. Xiao, and V. Vuletić, Near-unitary spin squeezing in ^{171}Yb, Phys. Rev. Lett. **122**, 223203 (2019).
[33] J. Estève, C. Gross, A. Weller, S. Giovanazzi, and M. K. Oberthaler, Squeezing and entanglement in a Bose–Einstein condensate, Nature (London) **455**, 1216 (2008).
[34] C. Gross, T. Zibold, E. Nicklas, J. Estève, and M. K. Oberthaler, Nonlinear atom interferometer surpasses classical precision limit, Nature (London) **464**, 1165 (2010).
[35] W. Muessel, H. Strobel, D. Linnemann, D. B. Hume, and M. K. Oberthaler, Scalable spin squeezing for quantum-enhanced magnetometry with Bose-Einstein condensates, Phys. Rev. Lett. **113**, 103004 (2014).
[36] D. M. Stamper-Kurn and M. Ueda, Spinor Bose gases: Symmetries, magnetism, and quantum dynamics, Rev. Mod. Phys. **85**, 1191 (2013).
[37] M. A. Kristensen, M. B. Christensen, M. Gajdacz, M. Iglicki, K. Pawłowski, C. Klempt, J. F. Sherson, K. Rzazewski, A. J. Hilliard, and J. J. Arlt, Observation of atom number fluctuations in a Bose-Einstein condensate, Phys. Rev. Lett. **122**, 163601 (2019).
[38] H. D. Politzer, Condensate fluctuations of a trapped, ideal Bose gas, Phys. Rev. A **54**, 5048 (1996).
[39] P. Navez, D. Bitouk, M. Gajda, Z. Idziaszek, and K. Rzażewski, Fourth statistical ensemble for the Bose-Einstein condensate, Phys. Rev. Lett. **79**, 1789 (1997).
[40] J. D. Sau, S. R. Leslie, M. L. Cohen, and D. M. Stamper-Kurn, Spin squeezing of high-spin, spatially extended quantum fields, New J. Phys. **12**, 085011 (2010).
[41] P. Kunkel, M. Prüfer, S. Lannig, R. Strohmaier, M. Gärttner, H. Strobel, and M. K. Oberthaler, Detecting entanglement structure in continuous many-body quantum systems, Phys. Rev. Lett. **128**, 020402 (2022).
[42] A. Kuzmich, N. P. Bigelow, and L. Mandel, Atomic quantum non-demolition measurements and squeezing, Europhys. Lett. **42**, 481 (1998).
[43] Y. Takahashi, K. Honda, N. Tanaka, K. Toyoda, K. Ishikawa, and T. Yabuzaki, Quantum nondemolition measurement of spin via the paramagnetic Faraday rotation, Phys. Rev. A **60**, 4974 (1999).
[44] K. Hammerer, K. Mølmer, E. S. Polzik, and J. I. Cirac, Light-matter quantum interface, Phys. Rev. A **70**, 044304 (2004).
[45] B. Q. Baragiola, L. M. Norris, E. Montaño, P. G. Mickelson, P. S. Jessen, and I. H. Deutsch, Three-dimensional light-matter interface for collective spin squeezing in atomic ensembles, Phys. Rev. A **89**, 033850 (2014).
[46] M. W. Mitchell and S. P. Alvarez, *Colloquium*: Quantum limits to the energy resolution of magnetic field sensors, Rev. Mod. Phys. **92**, 021001 (2020).
[47] P. J. Windpassinger, M. Kubasik, M. Koschorreck, A. Boisen, N. Kjærgaard, E. S. Polzik, and J. H. Müller, Ultra low-noise differential ac-coupled photodetector for sensitive pulse detection applications, Meas. Sci. Technol. **20**, 055301 (2009).
[48] F. M. Ciurana, G. Colangelo, R. J. Sewell, and M. W. Mitchell, Real-time shot-noise-limited differential photodetection for atomic quantum control, Opt. Lett. **41**, 2946 (2016).
[49] J. Takai, K. Shibata, N. Sekiguchi, and T. Hirano, Multistate interferometric measurement of the nonlinear ac Stark shift, Phys. Rev. A **107**, 053308 (2023).
[50] I. H. Deutsch and P. S. Jessen, Quantum control and measurement of atomic spins in polarization spectroscopy, Opt. Commun. **283**, 681 (2010).
[51] A. Steffen, W. Alt, M. Genske, D. Meschede, C. Robens, and A. Alberti, Note: *In situ* measurement of vacuum window birefringence by atomic spectroscopy, Rev. Sci. Instrum. **84**, 126103 (2013).
[52] A. A. Wood, L. D. Turner, and R. P. Anderson, Measurement and extinction of vector light shifts using interferometry of spinor condensates, Phys. Rev. A **94**, 052503 (2016).
[53] K. Shibata, N. Sekiguchi, and T. Hirano, Quantum lock-in detection of a vector light shift, Phys. Rev. A **103**, 043335 (2021).
[54] G. A. Smith, S. Chaudhury, A. Silberfarb, I. H. Deutsch, and P. S. Jessen, Continuous weak measurement and nonlinear dynamics in a cold spin ensemble, Phys. Rev. Lett. **93**, 163602 (2004).
[55] M. Koschorreck, M. Napolitano, B. Dubost, and M. W. Mitchell, Quantum nondemolition measurement of large-spin ensembles by dynamical decoupling, Phys. Rev. Lett. **105**, 093602 (2010).
[56] K. Burnett, P. S. Julienne, and K.-A. Suominen, Laser-driven collisions between atoms in a Bose-Einstein condensed gas, Phys. Rev. Lett. **77**, 1416 (1996).